Journal of Statistical Physics, Vol. 57, Nos. 5/6, 1989

Complexes of Block Copolymers in Solution: A Graph-Theoretical Approach

Ruud van Damme[1] **and Bernard J. Geurts**[2]

Received April 5, 1989; revision received July 17, 1989

We determine the statistical properties of block copolymers in solution. These complexes are assumed to have the topological structure of connected graphs with "nonnested" loops and cycles. The generating function method is used to determine the number of topologically different complexes containing a given number of block copolymers. It is shown that at sufficiently high concentration the system undergoes a transition to a gel phase. Furthermore, the average number of polymers per complex is calculated. Finally, the relative increase in viscosity is found under the assumption that the complexes can be treated as porous spheres.

KEY WORDS: Block copolymers; generating function method; Polya's theorem; gelation; nonnested structures.

1. INTRODUCTION

In a previous paper,[1] henceforth referred to as I, we started to apply the methods of equilibrium statistical physics to the study of block copolymer complexes in solution. The statistical properties of these complexes were determined under the assumption that the complexes have the topological structure of a tree. By assuming a definite topological structure for the complexes, the determination of various properties of the complexes could be mapped onto that of counting the number of topologically different complexes containing a certain number of block copolymers. The restriction to treelike structures was mainly based on mathematical convenience and not on a physical argument. Thus, we extend the treatment given in I

[1] Department of Applied Mathematics, Twente University, Enschede 7500 AE, The Netherlands.
[2] Center for Theoretical Physics, Twente University, Enschede 7500 AE, The Netherlands.

0022-4715/89/1200-1099$06.00/0

and include structures containing loops and cycles. Hence, we consider a considerably larger class of allowed topological structures accessible to the block copolymer complexes. The main implication of this extension is that the asymptotic behavior of the number of topologically different complexes, which depends on the number of polymers contained in them, is changed essentially when compared to the results based on the tree approximation. This has various consequences for the statistical properties of the complexes and provides experimentally testable differences. We determine the gelation boundary, the average number of block copolymers per complex, and the viscosity of the system, under the assumption that the complexes can be treated as porous spheres and hydrodynamic interactions are neglected. Also, we compare predictions for the statistical properties of the complexes with those obtained in I, which were based on the assxumption that the complexes have the topology of a tree. In view of the fact that the assumption about the topological structure of the complexes is ad hoc, in this and similar studies (e.g. refs. 2–4), we emphasize that sufficient care should be taken regarding this assumption since the predicxtions of the physical properties of the system depend sensitively on it.

The block copolymers considered can schematically be represented as ABA. The end groups (A) are much smaller than the connecting, linear and flexible polymers (B). The block copolymers are in solution and the solvent used is poor for the A parts and good for the B parts. Thus, the properties of this system are determined by two competing effects; on one hand, the A parts tend to leave the solution, but are hindered in doiing this by the fact that on the other hand the B parts tend to stay in solution. Hence, the A parts tend to cluster together in so-called "domains."[5] Larger complexes are formed consisting of a certain number of domains, connected by the B parts. Since the B parts are considered long and flexible, and the A parts tend to cluster in domains, it will be clear that physical equililbrium will be attained with complexes containing many loops and cycles. This is amplified by the fact that the number of topologically different complexes with loops and cycles increases much faster compared to the treelike complexes as a function of the number of block copolymers contained in them.

In I we derived the configuration sum $Q(\Gamma)$ of a system containing N block copolymers in solution in a volume V at thermodynamic equilibrium at temperature T. In this, Γ denotes a macrostate of the system; $\Gamma = (\gamma_1, \gamma_2, \ldots)$, where γ_k is the number of complexes containing k polymers. The configuration sum $Q(\Gamma)$ is required in order to determine the equilibrium size distribution of the complexes. We obtained

$$Q(\Gamma) = \prod_{k=1}^{N} (\gamma_k!)^{-1} v_k^{\gamma_k} \left(h^k \sum_{m=1}^{k+1} \sum_{\{n_j\}} T_{k,m,\{n_j\}} \prod_{j=1}^{2k} g_j^{n_j} \right)^{\gamma_k} \tag{1.1}$$

in which v_k is a translational combinatorial factor given by V/V_k, where V_k is the average volume occupied by a complex containing k polymers. The weight factor for a connecting B part is denoted by h and g_j is the weight factor associated with a domain containing j A parts. The functionality vector of a complex $\{n_j\}$ is defined such that n_j is the number of domains containing j A parts. Finally, $T_{k,m,\{n_j\}}$ is the number of topologically different complexes that can be formed with k polymers grouped such that there are m domains whose functionality vectors is $\{n_j\}$. If we take the "cluster energy" E_j to be additive, i.e.,

$$E_j = U_0 - (j-1)U_1; \qquad 0 < U_0 < U_1 \tag{1.2}$$

we find

$$g_j = g_1 \alpha^{j-1}; \qquad \alpha = \exp(U_1/k_B T) > 1 \tag{1.3}$$

and the configuration sum reduces to

$$Q(\Gamma) = \prod_{k=1}^{N} (\gamma_k!)^{-1} v_k^{\gamma_k} \left(\sum_{m=1}^{k+1} T_{k,m} (h\alpha^2)^k (g_1 \alpha^{-1})^m \right)^{\gamma_k} \tag{1.4}$$

where $T_{k,m}$ is the number of topologically different complexes with k polymers and m domains. The equilibrium distribution of the complexes Γ^* follows from maximizing $Q(\Gamma)$ subject to the constraint that Γ^* must be compatible. After some calculation one finds

$$\gamma_k^k = v_k (h\alpha^2 e^{-\lambda})^k \sum_{m=1}^{k+1} T_{k,m} \xi^m; \qquad \xi = \frac{g_1}{\alpha} < 1 \tag{1.5}$$

where λ is a Lagrange multiplier associated with the compatibility constraint

$$\sum_{k=1}^{N} k\gamma_k^* = N \tag{1.6}$$

The "Boltzmann" factor BF for a complex with k polymers and m domains is given by

$$\mathrm{BF} = (g_1 \alpha^{-1})^{\#\,\text{vertices}} (h\alpha^2)^{\#\,\text{edges}} \tag{1.7}$$

We can use Euler's identity, relating the number of vertices, edges, and loops/cycles (we will explain the difference between the latter two in Section 2),

$$\#\,\text{edges} + 1 = \#\,\text{vertices} + \#\,\text{loops/cycles} \tag{1.8}$$

to rewrite this as

$$\mathrm{BF} = (g_1 h\alpha)^{\#\,\text{vertices}} (h\alpha^2)^{\#\,\text{loops/cycles}\,-\,1} \tag{1.9}$$

The problem hence is to find the number of topologically different graphs, given the number of vertices and edges, or, equivalently, this number as a function of the number of vertices and loops/cycles. This specifies Γ^* completely. Various statistical properties of the complexes can then be expressed in terms of Γ^* and evaluated.

We concentrate on the effect of the possible formation of loops and cycles on the statistical properties of the system. The topological structure of the complexes will be such that loops and cycles are allowed. We restrict ourselves to a subset of all connected graphs, those that do not contain "nested" loops/cycles. We give a precise definition of these graphs in Section 2 and treat the corresponding counting problem in Section 3 by deriving functional equations for the relevant generating functions. Section 4 is devoted to a treatment of the asymptotic behavior of the number of complexes as a function of the number of vertices edges. In Section 5 we give a description of the numerical procedure used to evaluate this asymptotic behavior. Finally, in Section 6 we discuss the consequences for the statistical properties of the system and show that gelation occurs. Also, we calculate the viscosity of the system under the assumption that the complexes can be treated as porous spheres.

2. DEFINITION OF THE ALLOWED CLASS OF GRAPHS

In this section we first give a review of relevant definitions from graph theory. Next we introduce the set of allowed topological structures for the complexes, in which each edge in the graph corresponds to exactly one B part of a block copolymer.

A *graph* is a set of vbertices and edges (lines) connecting pairs of vertices. A *connected graph* is a graph such that for any two vertices of the graph there exists a path of edges belonging to the graph which connects those vertices. A *disconnected graph* is a graph which is not connected. A *rooted graph* is a graph in which a "root" is assigned to one of its vertices; one of the vertices is treated as a "base-point." A *line-rooted graph* is a graph with one of its edges defined as base-line; equivalently, such a root-line connects two adjacent root vertices. A *loop* consists of a single edge emanating from a vertex and returning to it. A *cycle* is a set containing at least two different edges and two different vertices. It is such that for any vertex in the cycle a path can be constructed emanating from that vertex and ultimately returning to it containing each edge of the cycle exactly once. In Fig. 1 we draw a loop, the smallest cycle, and a more complicated

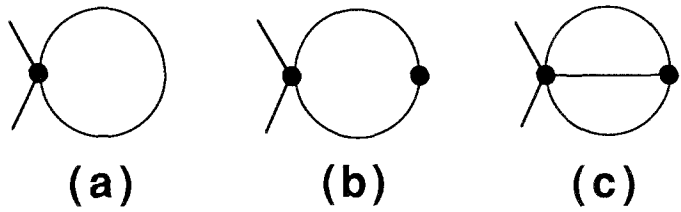

Fig. 1. Diagrams for (a) a loop, (b) the smallest cycle, and (c) an example of nested cycles.

structure containing three different nested cycles. Finally, a *bridge* is an edge which, when cut, renders a connected graph disconnected.

We next turn to the definition of the class of allowed graphs. Roughly speaking, a connected graph is "allowed" if it contains no nested cycles. In order to avoid pathologies, however, we define this class of graphs more precisely. We do this by defining a test for connected graphs, which allows one to discriminate between allowed and forbidden graphs. The procedure is as follows. Given an arbitrary connected graph, then: (1) contract all bridges, (2) omit all vertices with exactly two incident lines, and (3) omit all loops. Notice that the reduced graph of a tree consists of a single vertex, since all edges are bridges. In general the reduced graph consists of a certain number of connected cycles only. The graph we started the construction with is an element of the class of allowed graphs if the reduced graph is either a single vertex or if it is only "locally connected." By this we imply that if we cut an arbitrary edge of the reduced graph, then there is always another edge, which, when also cxut, renders the reduced graph disconnected. Stated differently, the functionality of each vertex in the reduced graph is even.

In Fig. 2 we show this test and find that the graph we started with is allowed. The graph in Fig. 3 does not meet the test (if one cuts l, there is no other line that could be cut, rendering the reduced graph disconnected).

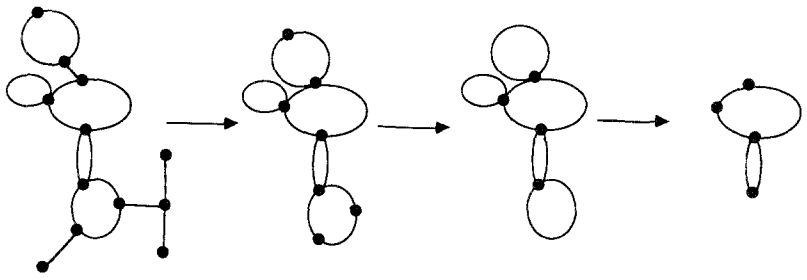

Fig. 2. The construction of the reduced graph for an allowed graph.

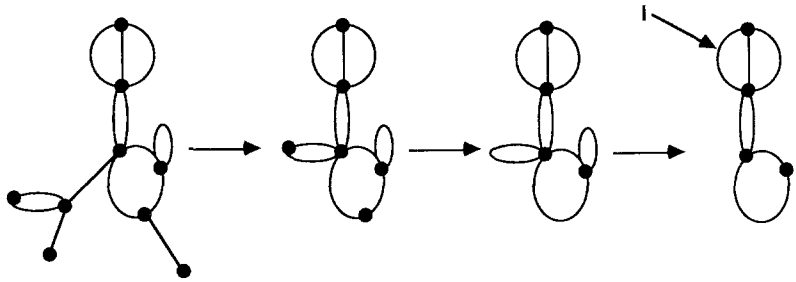

Fig. 3. This graph is not allowed, since if once cut l, there is no edge that when also cut renders the reduced graph disconnected.

In the next section we use the generating function method as based on Polya's theorem[6] in order to count the number of complexes containing k polymers grouped such that there are m domains. The allowed graphs will be mapped one-to-one onto a special type of tree and functional equations for the relevant generating functions will be derived.

3. COUNTING OF THE NUMBER OF ALLOWED GRAPHS

In this section we derive functional equations for the relevant generating functions to count the number of allowed topologically different structures. As we want to count graphs as a function of the number of vertices and loops/cycles, and as a function of the number of vertices and edges, we first derive a relation between the corresponding generating functions. Then, we derive a one-to-one correspondence between allowed graphs and a specific type of tree. These trees resemble so called "bicolored" trees.[6] We employ this correspondence to derive functional equations relating the generating functions for these trees to the generating functions for the graphs.

We first define the generating functions for the number of allowed graphs, counted as a function of the number of vertices and loops/cycles, and counted as a function of the number of vertices and edges. Then, we use Euler's identity to relate these two.

Let $S_{l,m}$ denote the number of graphs with l loops/cycles and m vertices (and consequently $l+m-1$ edges); then the generating function for these graphs is defined as

$$S(X, Y) = \sum_{m,l=0}^{\infty} S_{l,m} X^l Y^m \tag{3.1}$$

where we used counting variables X for the number of loops and cycles and Y for the number of vertices. Likewise, let, for the same graphs, $T_{k,m}$

denote the number of graphs with k edges and m vertices; then the corresponding generating function is given by

$$T(x, y) = \sum_{k,m=0}^{\infty} T_{k,m} x^k y^m \tag{3.2}$$

where x counts the edges and y the vertices. An important relation between T and S can be obtained using Euler's identity (1.8),

$$T(x, y) = x^{-1} S(x, xy) \tag{3.3}$$

which can be verified by substitution. This relation may be used if one wants to transform results in the "vertices and loop/cycle language," to the "vertices and edges language."

We will next relate the allowed graphs to a special type of bicolored tree, in a one-to-one correspondence. It is most expedient to do this for graphs ordered with respect to their number of vertices and loops/cycles and use (3.3) to chain the generating function $T(x, y)$. Consider an allowed graph and represent all vertices as "black." The construction of the corresponding bicolored tree then proceeds as follows: (1) put a new "white" vertex in the "center" of each loop/cycle (observe that this can be done in a unique way), (2) connect the black vertices which are on a loop/cycle with all their corresponding white vertices of those cycles (note that a black vertex may belong to more than one loop/cycle), and (3) omit all original edges which are not bridges. In Fig. 4 we draw an example of this procedure.

The resulting tree contains two types of vertices; the white vertices correspond to the original loops/cycles and the black vertices to the original vertices. Hence, two white vertices cannot be adjacent. Furthermore, a white vertex is at the end of a branch only if it represents a loop. The construction is one-to-one, i.e., each allowed graph corresponds to its

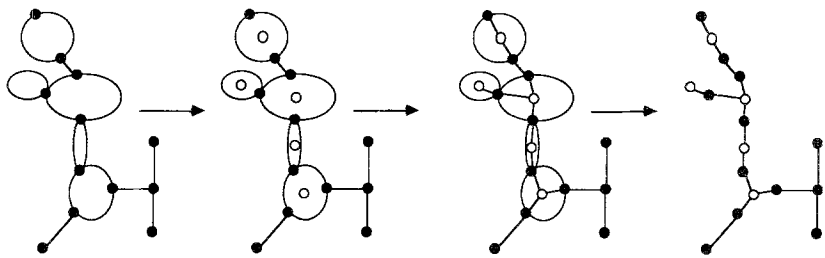

Fig. 4. The construction of the bicolored tree corresponding to the graph introduced in Fig. 2.

specific bicolored tree. It is also reversible if one keeps in mind the fact that the edges emanating from white vertices have a specific orientation, to which we return momentarily. In conclusion, we can state that counting the graphs as ordered to their number of vertices and loops/cycles is equivalent to counting the number of the bicolored trees introduced above. Using (3.3) then gives this number ordered with respect to the number of edges and vertices.

We will first count the number of bicolored trees rooted at a black and rooted at a white vertex. Then we unroot these trees to obtain $S(X, Y)$ and apply (3.3) to find $T(x, y)$. In the following we let $W(X, Y)$ denote the generating function for bicolored trees rooted at a white vertex and $B(X, Y)$ for those rooted at a black vertex.

Consider first a white-rooted tree. Obviously at least one line emanates from this vertex (a loop) and since two white vertices cannot be adjacent, all lines must connect to a black vertex. This is shown in the diagram in Fig. 5. As was explainded in detail in I, the proper way to count white-rooted trees is by taking the cycle index over the correct permutation group of the generating function [$B(X, Y)$ in this case]. The white vertices are special, in the sense that they possess orientation. This is explained in Fig. 6.

Hence, contrary to the treatment presented in I, we may not use the cycle index over S_n, the symmetric permutation group for the white-rooted trees. Rather, we must identify reflections and rotations, which are included in the so-called "dihedral" group D_n.[6] Thus, the diagram in Fig. 5 implies

$$W(X, Y) = X \sum_{n=1}^{\infty} Z(D_n, B(X, Y)) \tag{3.4}$$

where $Z(D_n, \cdot)$ is the cycle index over D_n. This can be expressed in closed form as[6]

$$Z(D_n, f) = \frac{1}{2n} \sum_{k|n} \varphi(k)\{f(x^k, y^k)\}^{n/k} + \frac{f(x, y)}{2}\{f(x^2, y^2)\}^{(n-1)/2} \tag{3.5}$$

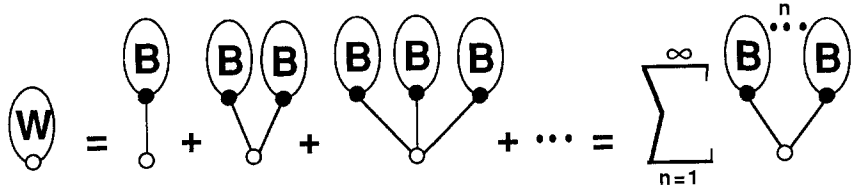

Fig. 5. Diagram for white-rooted trees (represented by a blob labeled W with a white dot) showing that all edges emanating from that vertex connect to a black-rooted tree (represented by a blob marked B with a black dot).

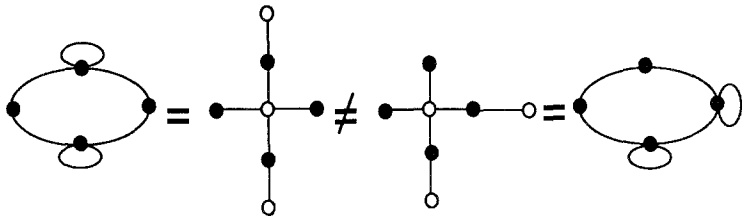

Fig. 6. Diagram indicating that not all permutations of the branches emanating from a white vertex result in identical structures.

if n is odd, and

$$Z(D_n, f) = \frac{1}{2n} \sum_{k|n} \varphi(k) \{f(x^k, y^k)\}^{n/k} + \frac{f(x^2, y^2) + f^2(x, y)}{4} \{f(x^2, y^2)\}^{(n-2)/2} \tag{3.6}$$

if n is even. In this φ is Euler's function[7] and $k|n$ denotes a sum over all k which divide n. Combination of the last three equations gives after some algebra

$$W_1 = -\frac{X}{2} \sum_{k=1}^{\infty} \frac{\varphi(k)}{k} \ln(1 - B_k) + \frac{X(B_1 + B_1^2/2 + B_2/2)}{2(1 - B_2)} \tag{3.7}$$

where we introduced the notation $W_k = W(X^k, Y^k)$ and $B_k = B(X^k, Y^k)$.

In an analogous way one can derive a functional equation for $B(X, Y)$. Observe that a black vertex may be connected to (i) another black vertex, (ii) a white vertex which represents a cycle, and (iii) a white vertex which represents a loop. The black vertices do not have an orientation, that is, any permutation of the branches emanating from a black vertex needs to be identified. Hence, we must use the cycle index over S_n. In Fig. 7 we draw the diagram for black-rooted trees.

From this diagram one obtains

$$B(X, Y) = Y \sum_{l,m,n=0}^{\infty} Z(S_n, B(X, Y))\, Z(S_m, W(X, Y))\, Z(S_l, X) \tag{3.8}$$

A central property of the cycle index taken over S_n is[6]

$$\sum_{n=0}^{\infty} Z(S_n, f) = \exp\left[\sum_{k=1}^{\infty} \frac{f(x^k, y^k)}{k}\right] \tag{3.9}$$

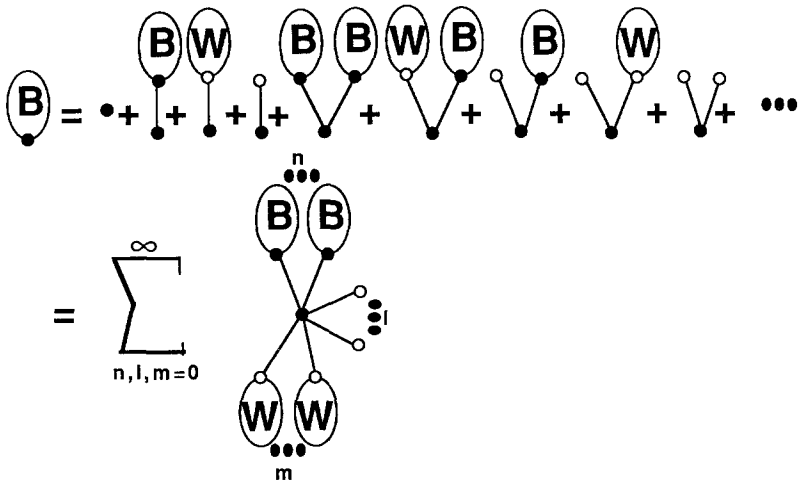

Fig. 7. Diagram for a black-rooted tree showing that a black vertex connects to an arbitrary number of black-rooted trees (n), an arbitrary number of loops (l), and an arbitrary number of white-rooted trees (m).

and thus as a special case

$$\sum_{l=0}^{\infty} Z(S_l, X) = \frac{1}{1-X} \tag{3.10}$$

Hence, (3.8) may be rewritten as

$$B_1 = \frac{Y}{1-X} \exp\left[\sum_{k=1}^{\infty} \frac{W_k + B_k}{k}\right] \tag{3.11}$$

The functional equations (3.7) and (3.11) together specify the generating functions W and B and hence the number of white- and black-rooted trees, given the number of white and black vertices in such a tree. Putting

$$B(X, Y) = Y + \text{higher orders}; \qquad W(X, Y) = XY + \text{higher orders} \tag{3.12}$$

we can iterate these equations and obtain for the first few terms, using the manipulation program REDUCE[8]:

$$B(X, Y) = Y(1 + X + X^2 + \cdots) + Y^2(1 + 3X + 5X^2 + \cdots) + Y^3(2 + 9X + \cdots) + \cdots \tag{3.13}$$

and

$$W(X, Y) = XY(1 + X + X^2 + \cdots) + X^2Y^2(2 + 4X + 7X^2 + \cdots) + X^3Y^3(4 + 14X + \cdots) + \cdots \tag{3.14}$$

It is left to the reader to verify these terms by drawing the corresponding diagrams. Figure 10 may be useful in doing this.

To conclude this section, we will express the generating functions S and T in terms of B and W. In view of the one-to-one correspondence between the bicolored trees and the allowed graphs, this implies that we obtain $S(X, Y)$ from unrooting the black- and white-rooted trees. In other words, $S(X, Y)$ is equal to the number of unrooted bicolored trees. Since we deal with trees, we can employ the unrooting procedure as explained in I. That is, the number of unrooted trees is equal to the number of rooted trees minus the number of line-rooted trees rooted at a nonsymmetry line. In Fig. 8 we draw a bicolored tree furnishing an example of this procedure.

So, we have

$$S(X, Y) = B(X, Y) + W(X, Y) - L_{B,W}(X, Y) \tag{3.15}$$

where $L_{B,W}$ is the generating function for bicolored trees rooted at a nonsymmetry line. Such a line-rooted tree can be generated by connecting the roots of black/white-rooted trees and black-rooted trees with loops (i.e., a single white vertex). This is shown in Fig. 9.

In counting line-rooted trees, one must identify reflections and permutations of the two objects connected. The reflections of two objects are included in the so-called "alternating" group A_2 and the permutations in S_2. An application of Poly's theorem[6] then gives

$$L_{B,W}(X, Y) = Z(A_2 - S_2, B + W + X) \tag{3.16}$$

where

$$Z(A_2 - S_2, f) = \tfrac{1}{2}[f^2(X, Y) - f(X^2, Y^2)] \tag{3.17}$$

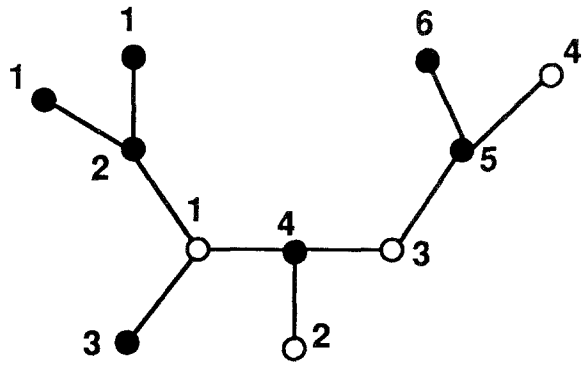

Fig. 8. A larger bicolored tree with 4 nonequivalent white vertices and 6 nonequivalent black vertices. The number of nonsymmetry lines is equal to 9.

Fig. 9. Diagram for line-rooted trees. Since two while vertices cannot be adjacent, the diagram in which a white-rooted tree is connected to a loop is absent.

A remark is in order with respect to (3.16), (3.17). In view of the fact that two white vertices cannot be adjacent, we may retain only the allowed terms as sketched in Fig. 9. Hence, cross-terms containing combinations of W and X as well as $W(X^2, Y^2)$ need to be omitted, since they correspond to "forbidden" connections of objects. We thus find

$$L_{B,W}(X, Y) = \tfrac{1}{2}[B^2(X, Y) - B(X^2, Y^2)] + B(X, Y)\, W(X, Y) + XB(X, Y) \tag{3.18}$$

and so, finally,

$$S(X, Y) = B(X, Y) + W(X, Y) - \tfrac{1}{2}[B^2(X, Y) - B(X^2, Y^2)] \\ B(X, Y)\, W(X, Y) - XB(X, Y) \tag{3.19}$$

Using (3.3), one hence obtains for $T(x, y)$

$$T(x, y) = \tilde{B}(x, y) + \tilde{W}(x, y) - \frac{x}{2}[\tilde{B}^2(x, y) - \tilde{B}(x^2, y^2)] \\ - x\tilde{B}(x, y)\, \tilde{W}(x, y) - x\tilde{B}(x, y) \tag{3.20}$$

where $\tilde{B}$ and $\tilde{W}$ are the generating functions for black/white-rooted trees ordered with respect to their number of black vertices and edges, i.e.,

$$\tilde{B}(x, y) = x^{-1}B(x, xy); \qquad \tilde{W}(x, y) = x^{-1}W(x, xy) \tag{3.21}$$

For the first few terms we obtain, using REDUCE,

$$T(x, y) = y(1 + x + x^2 + x^3 + \cdots) + y^2x(1 + 2x + 3x^2 + 4x^3 + \cdots) \\ + y^2x^2(1 + 4x + 9x^2 + \cdots) + \cdots \tag{3.22}$$

which can be verified using Fig. 10.

In summary, the allowed graphs can be mapped one-to-one onto bicolored trees in which an orientation has to be assigned to the "white" vertices, i.e., the loop/cycle representing vertices. The generating functions for black- and white-rooted trees, B and W, respectively, were determined and the correspondence between the bicolored trees and the allowed graphs

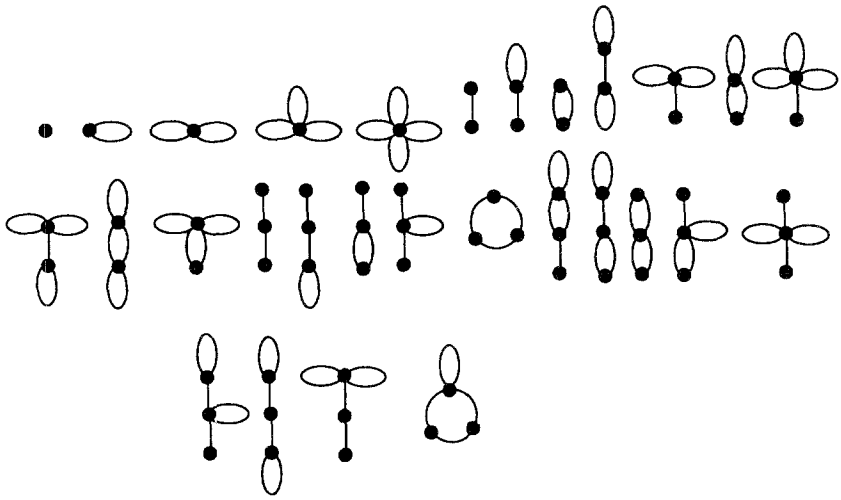

Fig. 10. All allowed graphs with up to three vertices and four edges.

was employed to express the generating functions for these graphs in terms of B and W.

In a completely analogous way, the generating functions for an extended class of graphs can be derived. One allows the edges in the graph to represent an arbitrary number of block copolymers. The derivation is similar to the one given above with some small alterations. As was shown in I, this "line-dressed" case is dominated by the, in principle, unbounded number of connections between two neighboring vertices. Such options are, however, somewhat artificial, since steric hindrance effects and packing limitations obviously imply a maximum to the number of polymers between two neighboring domains. We will not pursue this case here.

In the next section we analyze the singular behavior of the generating functions derived above. This results in the asymptotic dependence of the number of graphs on the number of edges.

4. ANALYSIS OF THE SINGULAR BEHAVIOR OF THE GENERATING FUNCTIONS

First we derive the singular behavior of $B(X, Y)$ and investigate the consequences for the other generating functions later. In particular, we will prove in detail that $T(x, y)$ has a square root singular behavior which is essentially different from the behavior of the generating function for treelike structures discussed in I.

In view of (3.7), (3.11), we introduce the function

$$\mathscr{H}(\zeta, X, Y)=\frac{Y}{1-X}\exp\left\{\left[\zeta+\frac{X}{2}\left(\frac{\zeta(1+\zeta)/2}{1-B_2}-\ln(1-\zeta)\right)\right]+h(X, Y)\right\}-\zeta \tag{4.1}$$

where

$$h(X, Y)=\frac{XB_2}{4(1-B_2)}-\frac{X}{2}\sum_{n=2}^{\infty}\frac{\varphi(n)}{n}\ln(1-B_n)$$
$$\times\sum_{l=2}^{\infty}\frac{1}{l}\left\{B_l+\frac{X^l}{2}\left[\frac{B_l+(B_l^2+B_{2l})/2}{1-B_{2l}}-\sum_{n=1}^{\infty}\frac{\varphi(n)}{n}\ln(1-B_{nl})\right]\right\} \tag{4.2}$$

Clearly $\mathscr{H}(B(X, Y), X, Y)=0$ and hence $B(X, Y)$ can be expanded in a Taylor series unless

$$\mathscr{H}_\zeta(B(X, Y), X, Y)=0 \tag{4.3}$$

which defines, together with $\mathscr{H}=0$, the singular line for the generating function $B(X, Y)$. In the sequel we keep $0<Y<1$, Y fixed, and denote the singular line by $R(Y)$. Moreover, we put $F_0\equiv B(R(Y), Y)$ for notational convenience. At the singular point $(R(Y), Y)$ condition (4.3) implies, after some rewriting,

$$F_0\left[1+\frac{1}{2}R(Y)\left(\frac{1+F_0}{1-B_2^R}+\frac{1}{1-F_0}\right)\right]=1 \tag{4.4}$$

In addition, one may show that

$$\mathscr{H}_{\zeta\zeta}(F_0, R(Y), Y)=\frac{1}{F_0}+\frac{1}{2}F_0R(Y)\left(1+\frac{1}{(1-F_0)^2}\right) \tag{4.5}$$

and so $\mathscr{H}_{\zeta\zeta}\neq 0$. Thus, for X close to but smaller than $R(Y)$, the generating function B can be expanded as

$$B(X, Y)=F_0-F_1\Delta^{1/2}+F_2\Delta+\cdots \tag{4.6}$$

where we put $\Delta=R(Y)-X$ and it is understood that the "expansion functions" $F_i=F_i(Y)$. The function F_1 can be shown to be given by

$$F_1=\lim_{X\uparrow R(Y)}\left(\frac{2\mathscr{H}_X(B(X, Y), X, Y)}{\mathscr{H}_{\zeta\zeta}(B(X, Y), X, Y)}\right)^{1/2} \tag{4.7}$$

We defer the determination of estimates of F_0, F_1, and $R(Y)$ to the next section and proceed with the consequences of (4.6) for the other generating functions introduced in the previous section.

The generating function for white-rooted trees $W(X, Y)$ can be expanded as

$$W(X, Y) = G_0 - G_1 \Delta^{1/2} + \cdots \tag{4.8}$$

where we put $G_0 = W(R(Y), Y)$ and G_1 is given by

$$G_1 = \frac{1}{2} R(Y) F_1 \left(\frac{1 + F_0}{1 - B_2^R} + \frac{1}{1 - F_0} \right) = F_1 \frac{1 - F_0}{F_0} \tag{4.9}$$

where use was made of (4.4). Inserting (4.6) and (4.8) into (3.19), one may show that

$$S(X, Y) = E_0(Y) - E_1(Y) \Delta^{1/2} + \cdots \tag{4.10}$$

with $E_0(Y) = S(R(Y), Y)$ and

$$E_1(Y) = (F_1 + G_1)(1 - F_0) - F_1[G_0 + R(Y)] \tag{4.11}$$

The expansion for $T(x, y)$ can be shown to be given by

$$T(x, y) = \frac{E_0(Y)}{R(Y)} - \frac{E_1(Y)}{R(Y)} \tilde{\Delta}^{1/2} + \cdots; \qquad \tilde{\Delta} \equiv R(Y) - x \tag{4.12}$$

where use was made of (3.3). In this, the values of y and Y are found to be related by

$$Y = yR(Y) \tag{4.13}$$

which stems from the identification (3.3). In summary, we may state that all generating functions considered have a square root singular term and in particular this implies that asymptotically

$$\sum_{m=1}^{k+1} T_{k,m} y^m \approx \frac{E_1(Y) R^{1/2}(Y)}{2\sqrt{\pi}} R^{-(k+1)}(Y) k^{-3/2} \tag{4.14}$$

The essential difference between this result and the corresponding result for treelike structures is the appearence of $k^{-3/2}$ rather than $k^{-5/2}$ as found in I. This has various implications for the statistical properties of the block copolymer complexes which be discussed in Section 6. We may state at this point, however, that the assumption made for the topological structure of

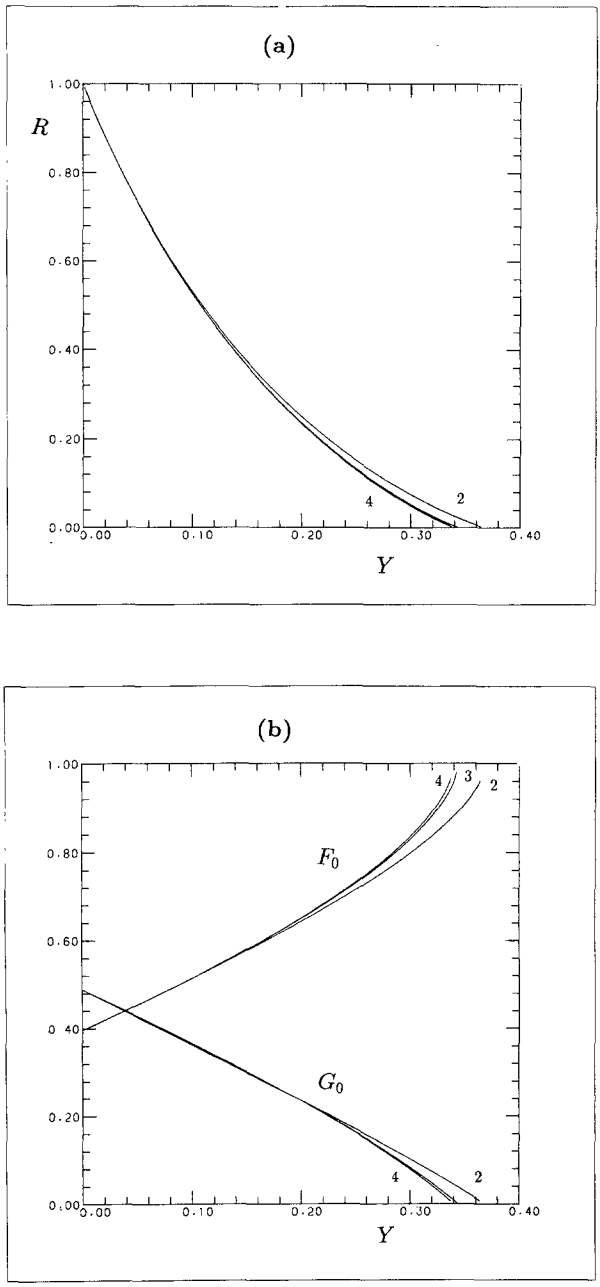

Fig. 11. Estimates for (a) R and (b) F_0, G_0 obtained by setting $B_n^R = 0$ for $n \geqslant \tilde{n} = 2, 3, 4$. The corresponding value of $\tilde{n}$ is indicated near the corresponding curve.

the complexes has a decisive influence on the statistical properties of those complexes. Since that assumption about the structure is largely ad hoc in most vases, we emphasize that sufficient care should be taken in similar analyses as to this assumption. In order to complete the derivation of the asymptotic behavior (4.14), we show that $E_1(Y) \neq 0$ in the Appendix.

In the next section we describe the procedure used in order to obtain estimates for the desired functions, in particular $E_1(Y)$ and $R(Y)$, which specify the asymptotic behavior (4.14).

5. NUMERICAL ANALYSIS OF THE ASYMPTOTIC BEHAVIOR

In order to get numerical estimates for the "expansion functions" introduced in Eqs. (4.6), (4.8), and (4.10), we use a consequence of the upper bound (A.4) derived in the Appendix on B_n^R. Since $F_0 < 1$, we notice that $B_n^R < e^{-n}$ for $n = 2, 3, \ldots$. Hence, we may approximate the infinite set of equations governing F_0 and B_n^R as given by (3.11) by a finite one in which we put $B_n^R = 0$ for n larger than some cutoff value $\tilde{n}$. The resulting approximate problem then consists of a finite system of nonlinear equations in the unknowns $\{F_0, B_n^R; n \leqslant \tilde{n}\}$, which may be solved numerically using standard techniques. The results thus obtained for $R(Y)$, F_0, and G_0 are shown in Fig. 11. Notice that the estimates to these functions appear to be very rapidly converging. Furthermore, the critical Y value above which no solution exists is given by the convergence radius of the generating function for normal trees, treated in I. Finally, in view of the identification (4.13) and the fact that we restrict ourselves to $y < 1$, we observe that the required value of Y corresponding to $y < 1$ are smaller than 0.2 approximately. However, in that region already the lowest order approximation is quite accurate and hence we will use only this lowest order in our subsequent calculations. Also, an improvement of the estimates for these functions by increasing the order of approximation is somewhat artificial, since in the asymptotic behavior (4.14) we restricted ourselves to the leading order.

In order to obtain an estimate of the function $E_1(Y)$, an evaluation of F_1 as given by (4.7) is required. In lowest order we obtain after some calculation

$$\mathscr{H}_X(F_0, R(Y), Y) = F_0 \left[\frac{1}{1 - R(Y)} + \frac{1}{2} F_0 \left(1 + \frac{1}{2} F_0 \right) - \frac{1}{2} \ln(1 - F_0) \right] \tag{5.1}$$

and thus F_1 is expressed in terms of F_0 and $R(Y)$, for which we have accurate estimates. In Fig. 12 we plot $E_1(Y) R^{1/2}(Y)$ as found in this approximation. This is a monotonically increasing function of Y which

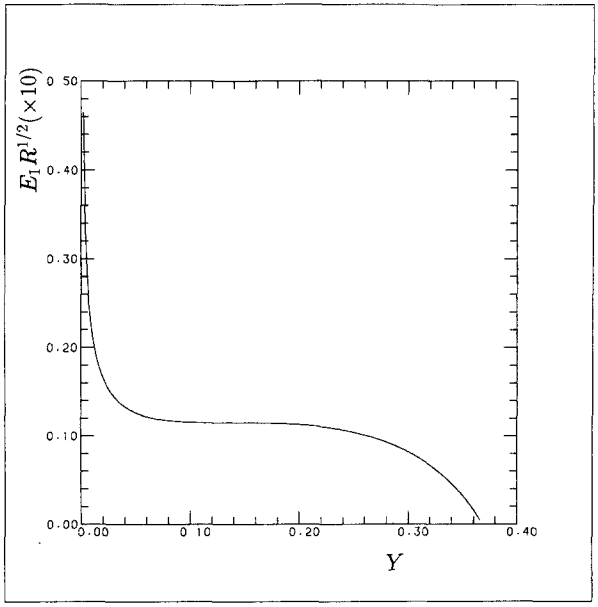

Fig. 12. Lowest order approximation to the "expansion function" $E_1(Y)\, R^{1/2}(Y)$.

shows a sharp increase as Y tends to zero. In view of (5.1) and the fact that $R(Y)$ is regular for $Y \ll 1$, we find after some calculation that $E_1(Y) \sim Y^{-1/2}$ as $Y \ll 1$. The implications of this singularity for the statistical properties of the complexes will be investigated in the next section.

6. STATISTICAL PROPERTIES OF BLOCK COPOLYMER COMPLEXES

In this section we employ the asymptotic results obtained in Section 4 to predict the statistical properties of the complexes and investigate the conditions under which a gelation transition occurs, i.e., the situations in which an organization of the polymers in finite complexes cannot be realized. Then we determine the density dependence of the average number of polymers in a complex. Finally, we calculate the relative increase in the viscosity of this system, treating the complexes as porous spheres and disregarding hydrodynamic interaction between the complexes.

The size distribution of the complexes is given by (1.5). Combination of this with (4.14) gives

$$\gamma_k^* = v_k (h\alpha^2 e^{-\lambda})^k \frac{E_1(Y)\, R^{1/2}(Y)}{2\sqrt{\pi}} R^{-(k+1)}(Y) k^{-3/2} \tag{6.1}$$

in which it is understood that Y satisfies $Y = \xi R(Y)$, defining Y as a function of ξ. As was argued in I, the translational factor v_k can be expressed as $v_k = v_0 k^{-\beta}$, in which $v_0 \equiv V/V_0$, with V_0 a volume associated with the volume occupied by a single block copolymer in solution. Hence,

$$\gamma_k^* = \frac{\chi(Y) v_0}{R(Y)} k^{-(\beta + 3/2)} z^k \tag{6.2}$$

where

$$\chi(Y) = \frac{E_1(Y) R^{1/2}(Y)}{2\sqrt{\pi}}; \qquad z = \frac{h\alpha^2 e^{-\lambda}}{R(Y)} \tag{6.3}$$

The value for z follows from the constraint (1.6), which results in

$$\sum_{k=1}^{\infty} k^{-(\beta + 1/2)} z^k = \frac{R(Y)}{\chi(Y)} V_0 \rho \equiv \rho_1 \tag{6.4}$$

where ρ is the polymer density, $\rho = N/V$. The left-hand side of (6.4) has a convergence radius equal to 1 and if $0 \leqslant \beta \leqslant 1/2$, this series is unbounded, whereas it is bounded if $\beta > 1/2$.

The critical volume fraction $(V_0\rho)_c$, defined as the volume fraction above which the system is in the gel state, as a function of β and ξ is thus given by

$$(V_0\rho)_c = \frac{\chi(Y)}{R(Y)} \sum_{k=1}^{\infty} k^{-(\beta + 1/2)}; \qquad Y = \xi R(Y) \tag{6.5}$$

Since the natural upper bound on $(V_0\rho)_c$ is 1 we thus find that the system shows gelation at sufficiently high concentration and/or sufficiently low temperature at some β and ξ values if the right-hand side becomes smaller than 1. Hence, if $0 \leqslant \beta \leqslant 1/2$, the system does not show a gelation transition. Also, since $\chi(Y) \sim Y^{-1/2} \sim \xi^{-1/2}$ if $\xi \ll 1$, there is no gelation if $\beta > 1/2$ at sufficiently low ξ values. Apparently, a large binding energy together with the increased number of different complexes as compared to the tree approximation implies that the system does not form a gel, but rather organizes into complexes of a finite size. In Fig. 13 we plotted some gelation boundaries as a function of β at various ξ values.

In order to specify a measure for the average size of the complexes, we next consider $\langle k \rangle$, the average number of block copolymers per complex. This quantity is given by

$$\langle k \rangle = \frac{\sum_{k=1}^{\infty} k\gamma_k^*}{\sum_{k=1}^{\infty} \gamma_k^*} = \frac{\sum_{k=1}^{\infty} k^{-(\beta + 1/2)} z^k}{\sum_{k=1}^{\infty} k^{-(\beta + 3/2)} z^k} \tag{6.6}$$

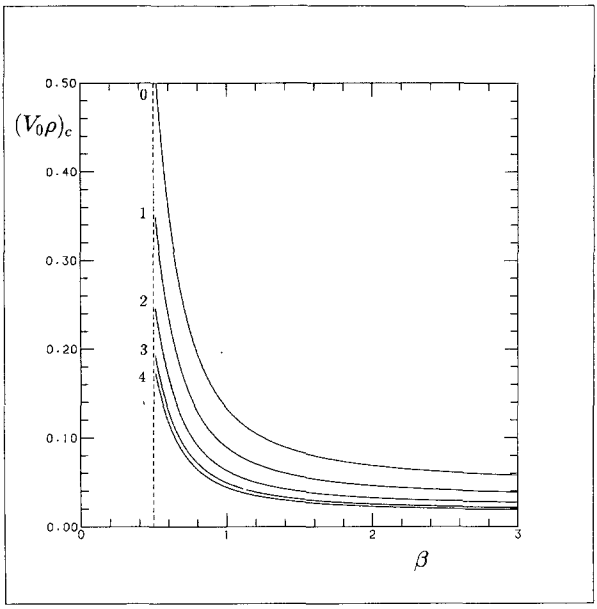

Fig. 13. Plot of the critical volume fraction $(V_0\rho)_c$ as a function of β for various ξ values. We use $\xi = 2^{-j}$ and indicate the values of j near the corresponding curve.

where z satisfies (6.4). Notice that $\langle k \rangle$ can become unbounded if $0 \leqslant \beta \leqslant 1/2$ and it is bounded if $\beta > 1/2$. In Fig. 14 we show $\langle k \rangle$ as a function of ρ_1 at various β values. As β increases ($\beta > 1/2$), gelation sets in earlier and the maximal value for $\langle k \rangle$ decreases. Furthermore, the increase in $\langle k \rangle$ is smaller at small ρ_1 values as β increases and larger close to the corresponding gelation value. In comparison with the results obtained based on the tree approximation, we find much higher values of $\langle k \rangle$. Together with the fact that the size distribution of the complexes has a "longer tail" when compared to the tree approximation ($k^{-3/2}$ and $k^{-5/2}$, respectively), we notice that the assumption required about the topological structure of the complexes has an essential influence on the predicted physical properties.

Finally, we turn to the determination of the viscosity of the solution. In I we have shown, closely following Felderhof,[9] that if hydrodynamic interactions between different complexes are disregarded and the complexes are treated as porous spheres, the relative increase in viscosity may be expressed as

$$\frac{\eta - \eta_0}{\eta_0} = \frac{5\chi(Y)}{2R(Y)} \sum_{k=1}^{\infty} z^k k^{-3/2} \frac{H(\sigma_k)}{1 + 10H(\sigma_k)/\sigma_k^2} \tag{6.7}$$

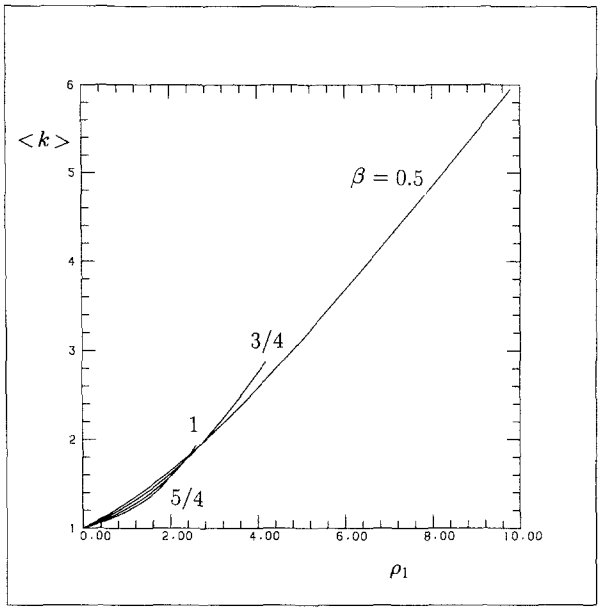

Fig. 14. The average number of block copolymers per complex as a function of ρ_1 for some β valules indicated near the corresponding curve.

where η_0 is the viscosity of the solvent, η the viscosity of the solution, and

$$H(\sigma_k) = 1 + \frac{3}{\sigma_k^2} - \frac{3}{\sigma_k}\coth(\sigma_k) \tag{6.8}$$

where

$$\sigma_k = \mathscr{B}k^{(1-\beta/3)/2}; \qquad \mathscr{B} \equiv \left(\frac{2\phi M^{1-\mu}}{4\pi a \eta_0}\right)^{1/2} \tag{6.9}$$

In the expression for $\mathscr{B}$ we put ϕ for the friction coefficient of the segments of the B parts of the block co-polymers with the medium, M for the number of segments constituting those B parts, and a the segment step length. Finally, μ is Flory's constant[10] ($\mu \approx 3/5$) describing the polymer statistics of the B parts in good solvents, i.e., with excluded volume interactions to be included. In Fig. 15 we plot $R(Y)(\eta - \eta_0)/\chi(Y)\eta_0$ versus ρ_1 at various $\mathscr{B}$ and β values. The increase in viscosity at low ρ_1 values is roughly independent of β and is mainly determined by $\mathscr{B}$. The high-density regime, however, does depend sensitively on β. In view of the behavior of $\chi(Y)$ as Y becomes small, we notice that at realistic values of ξ ($\ll 1$) the actual increase in $(\eta - \eta_0)/\eta_0$ becomes very large. This can be understood

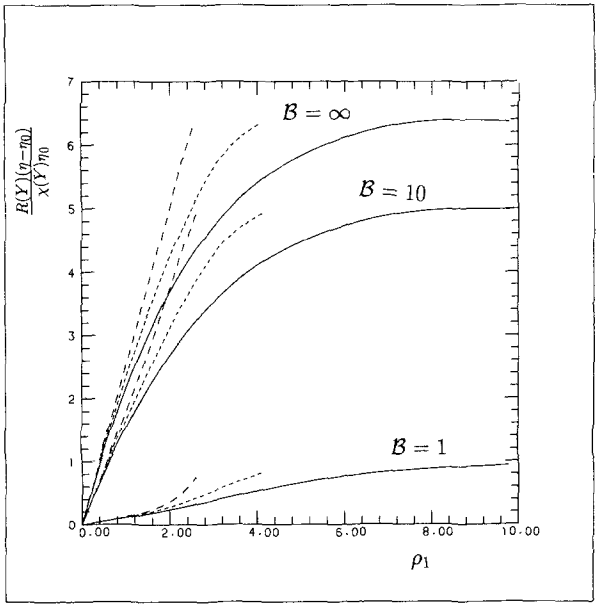

Fig. 15. Plot of $R(Y)(\eta-\eta_0)/\chi(Y)\eta_0$ versus ρ_1 at various $\mathcal{B}$ values, which are indicated near the corresponding curves. The solid curves correspond to $\beta=0.5$, the short-dashed curves to $\beta=0.75$, and the long-dashed curves to $\beta=1$.

from the fact that in this regime the average complex size is quite large. In our treatment these larger complexes are less permeable and their contribution to the increase in viscosity is larger.

In order to compare the predictions for $\langle k\rangle$ and $(\eta-\eta_0)/\eta_0$ obtained above and those obtained in I for complexes having the structure of a tree, we relate the quantities shown graphically in both cases. In I we used $\rho^* \sim V_0\rho/\xi$ as variable to represent the polymer density. Compared to ρ_1 used above, we notice that in realistic cases ($\xi \ll 1$) we have $\rho_1 \ll \rho^*$. Also, $R(Y)/\chi(Y) \sim \xi^{-1/2}$ in this regime, as may be inferred from (6.3). Hence, when regarded as a function of ρ^* we have that $\langle k\rangle$ can become much lmarger for structures with loops and cycles, but increases much more slowly when compared to treelike structures treated in I. Finally, the increase in viscosity as characterised by the intrinsic viscosity is much larger for structures containing loops and cycles.

APPENDIX

In order to show that $E_1(Y)$ is not identically zero, we construct a lower bound to $E_1(Y)$ and show this bound to be positive. Insertion of (4.9) into (4.10) yields

$$E_1(Y) = F_1\left[\frac{1}{F_0} - 1 - G_0 - R(Y)\right] \tag{A.1}$$

Since "black-rooted" trees contain as a special case also the normal trees, one infers $F_1 \neq 0$ and hence we may restrict ourselves to the term between square brackets. We will derive accurate upper bounds on G_0 and $R(Y)$ in terms of F_0 and show that this term is positive on the interval [0, 1], thus completing the proof. We start with G_0, which is given by

$$G_0 = \frac{R(Y)}{2}\left(\frac{F_0 + (F_0^2 - B_2^R)/2}{1 - B_2^R} - \sum_{n=1}^{\infty} \frac{\varphi(n)}{n} \ln(1 - B_n^R)\right) \tag{A.2}$$

where we introduced the notation $B_n^R = B(R^n(Y), Y^n)$. Using (3.11), we have

$$\begin{aligned} \ln(B_n^R) &= n \ln(Y) - \ln[1 - R^n(Y)] + \sum_{k=1}^{\infty} \frac{B_{kn}^R + W_{kn}^R}{k} \\ &< n\{\ln(F_0) - F_0\} + \sum_{k=2}^{\infty}{}' \frac{1}{k}(B_{kn}^R - nB_n^R + W_{kn}^R - nW_n^R) \end{aligned} \tag{A.3}$$

where the prime on the summation indicates that $k \neq n^j$, $j = 1, 2, \ldots$. Since $B_n^R \geqslant B_{nk}^R$ and $W_n^R \geqslant W_{kn}^R$, we thus obtain

$$B_n^R < [F_0 e^{F_0}]^n \tag{A.4}$$

Insertion into (A.2) yields

$$\begin{aligned} G_0 < \frac{R(Y)}{2}\Bigg[&\frac{F_0 + (F_0^2/2)(1 + e^{-2F_0})]}{1 - F_0^2 e^{-2F_0}} \\ &+ \frac{F_0 e^{-F_0}}{1 - F_0 e^{-F_0}} + \ln \frac{1 - F_0 e^{-F_0}}{1 - F_0}\Bigg] \end{aligned} \tag{A.5}$$

where use was made of [7]

$$\begin{aligned} \sum_{k=1}^{\infty} \varphi(k) \frac{x^k}{1 - x^k} &= \frac{x}{(1-x)^2} \\ \sum_{k=1}^{\infty} \frac{\varphi(k)}{k} \ln(1 - x^k) &= -\frac{x}{1-x} \end{aligned} \tag{A.6}$$

We finally derive an upper bound on $R(Y)$ in terms of F_0. Solving $R(Y)$ from (4.4) gives

$$R(Y) = 2\frac{(1-F_0)^2(1-B_2^R)}{F_0(2-F_0^2-B_2^R)} \tag{A.7}$$

One readily obtains the lower bound

$$B_2^R > \frac{Y^2}{1-R^2(Y)} \tag{A.8}$$

using (3.11), and hence the combination of (A.7) with (A.4) and (A.8) results in

$$-R^3(Y) + \mathscr{A}R^2(Y) + R(Y) - \mathscr{A}(1-Y^2) < 0 \tag{A.9}$$

where

$$\mathscr{A} \equiv 2\frac{(1-F_0)^2}{F_0[2-F_0^2(1+e^{-2F_0})]} \tag{A.10}$$

Thus, guided by (A.9) also

$$\mathscr{A}R^2(Y) + R(Y) - \mathscr{A} < 0 \tag{A.11}$$

and so

$$R(Y) < \frac{-1+(1+4\mathscr{A}^2)^{1/2}}{2\mathscr{A}} \tag{A.12}$$

Insertion of (A.5) and (A.12) into (A.1) gives a rather complicated expression in terms of F_0. Evaluation of this expression for $0 < F_0 < 1$ shows that it is positive and hence the proof is completed.

REFERENCES

1. B. J. Geurts and R. van Damme, *J. Stat. Phys.* **57**:1069 (1989).
2. F. W. Wiegel and A. S. Perelson, *J. Stat. Phys.* **29**:813 (1982).
3. F. W. Wiegel, B. J. Geurts, and B. Goldstein, *J. Phys. A: Math. Gen.* **20**:5205 (1987).
4. J. Spouge, *J. Stat. Phys.* **43**:143 (1986).
5. K. Visscher and P. F. Mijnlieff, In preparation (1989).
6. P. Harary and F. Palmer, *Graphical Enumeration* (Academic Press, 1973).
7. M. Abramowitz and I. A. Stegun, *Handbook of Mathematical Functions* (Dover, New York, 1964).
8. A. C. Hearn, *REDUCE User's Manual* (Rand, 1983).
9. B. U. Felderhof, *Physica* **80A**:172 (1975).
10. P. G. de Gennes, *Scaling Concepts in Polymer Physics* (Cornell University Press, 1979).